Mixed Field Dosimetry Using Focused and Unfocused Laser Heating of Thermoluminescent Materials

Final Report
(Covering Period from April 15, 1992 to June 30, 1995)

Grant No. DE-FG05-93ER75879

Prepared by: Dr. C-K Chris Wang

Date: July 24, 1995

This work had as its original goals the theoretical evaluation of a unique method of performing mixed field dosimetry by using focused and unfocused laser heating to extract dose information from the superficial layers, followed by the deeper layers, of a single, thick thermoluminescent detector (TLD). This report will review the original stated goals for this award, then review the results obtained during the three years of grant period.

TABLE OF CONTENTS

Mixed Field Dosimetry Using Focused and Unfocused Laser Heating of Thermoluminescent Materials

Project Objectives and Goals

The objective of the research project is to develop a unique dosimetry system capable of accurately assessing mixed beta/gamma dosimetry and meaningful shallow/deep dose discrimination using a single-element thermoluminescent detector (TLD) and focused laser readout. The rapid superficial heating of a thick TLD will result in release of the signal due to shallow dose, which will then be followed by the release of the signal due to the deep dose as the deeper portions of the TLD are heated to TL temperatures. The basic hypothesis is that this approach will prove superior to the approaches of employing thin dosimeters, multi-element filtered dosimeters with empirical algorithms, and rapid superficial contact heating. The major goal of the research is to explore this basic hypothesis using computer simulations of the laser heating and thermoluminescent processes.

Specific project objectives, presented in the original proposal, are:

1) Theoretical analysis of signal or glow curve production in a TLD undergoing superficial heating with a focused laser;

2) Characterization of the glow curve for TLDs heated by a focused laser followed by unfocused laser heating;

3) Optimal selection of TLD type, dimensions and heating scheme for discrimination of beta and gamma dose;

4) Optimization of the approach for characterizing the depth of penetration of beta fields; and

5) Specification of a prototype system.

Results and Discussion

Software tools required for accomplishing the specific objectives were essentially developed during the first year of the grant. Preliminary simulations obtained suggested a modified approach to the problem, namely the use of a uniform laser beam and a laser pulse sequence for heating

coupled with a deconvolution technique applied to the resulting glow curves in order to determine the depth dose. All five goals have been achieved. The detailed description of the modified approach and the simulated results are provided in Attachment A. In summary, the modified approach appears to be novel and feasible. However, the deconvoluted depth-dose result may contain large uncertainties due to the uncertainties associated with the thermal parameters of TLD, namely absorption coefficient of laser beam, thermal conductivity, and specific heat. To thoroughly address this issue, an experimental study must be conducted.

THEORETICAL EVALUATION OF MIXED BETA/GAMMA FIELD DOSIMETRY USING PULSED LASER HEATING OF THERMOLUMINESCENT MATERIALS

C.-K. Chris Wang[1], Seungjae Han[1], and K.J. Kearfott[1]

[1] Georgia Institute of Technology, Health Physics Program,
School of Mechanical Engineering, Atlanta, GA 30332-0225, USA

[1] University of Michigan, Department of Nuclear Engineering,
Cooley Laboratory, North Campus, Ann Arbor, MI 48109, USA

Short Title:
Pulsed Laser heating of TLDs

THEORETICAL EVALUATION OF MIXED BETA/GAMMA FIELD DOSIMETRY USING PULSED LASER HEATING OF THERMOLUMINESCENT MATERIALS

C.-K. Chris Wang, Seungjae Han, and K.J. Kearfott

Abstract -- This paper described a detailed computational study of a new method for mixed beta/gamma radiation field dosimetry using single-element thermoluminescent dosemeters (TLD) with pulsed laser heating schemes. The main objective of this study was to obtain an optimum heating scheme so that the depth-dose distribution in a thick TLD could be determined. The major parts of the study include: (1) heat conduction calculations for TLDs with various heating schemes, (2) glow curve calculations for TLDs, (3) unfolding of the depth-dose distribution based on the glow curve data, and (4) estimation of shallow and deep dose from the unfolded depth-dose distribution. An optimum heating scheme based on a sequence of laser pulses were obtained in this study for a uniform laser beam. The resulting glow curves were successfully used to unfold the depth-dose distribution in the TLD. The unfolded depth-dose distribution correctly predicts the shallow and deep doses with relative errors less than 20% in various pure and mixed beta/gamma radiation fields.

INTRODUCTION

Mixed beta/gamma dosimetry typically involves determining the shallow (or skin) dose and deep dose for human body exposed to mixed beta/gamma radiation fields. The International Commission on Radiological Protection (ICRP)[1] has recommended that an appropriate measurement of skin dose is that integrated between tissue depths of 5 and 10 $mg.cm^{-2}$ (i.e. 50-100 μm) which corresponds to the depth of cells in the basal layer of the body. More recently, the International Commission on Radiological Units and Measurement (ICRU)[2] prescribed two new operational quantities intended for application to individual monitoring: the individual dose equivalent penetrating, $H_p(d)$, and individual dose equivalent superficial, $H_s(d)$. They are defined as the dose equivalent in soft tissue below a specified point on the body at depths of 10.0 and 0.07 mm, respectively. Two major techniques have been attempted to measure these quantities using thermoluminescent dosimeters (TLDs). They include using thin detectors and multi-element dosimeters.

A thin TLD typically has a thickness of approximately 5 $mg.cm^{-2}$. To measure $H_s(d)$ and $H_p(d)$, tissue-equivalent filters with thicknesses of 7 $mg.cm^{-2}$ and 1.0 $g.cm^{-2}$ must be used respectively. Several types of thin TLDs have been developed[3,4]. The materials include $CaSO_4$(Tm), MgB_4O_7(Tm), and LiF(Mg,Cu,P). The first two materials are regarded as ceramic TLDs, and their sensitivity to mixed beta/gamma radiation are higher than that of the LiF(Mg,Cu,P). The ceramic TLDs are less tissue-equivalent, however, and require corrections of the over-response at low photon energies.

In the multi-element approach, a minimum of three detectors, two for shallow dose and one for deep dose, are placed behind different thickness of filters. The resulting readings for the various detectors are then analyzed to evaluate shallow dose and deep dose equivalents[5,6]. The ultimate limitations of this approach are discontinuities and instabilities of the computational algorithms, the system energy dependence, the low limit for the measurable maximum beta energy, the high lower limit of detectability, and added cost due to the use of multiple detectors[7,8]. In addition, dosimeter-to-dosimeter variation introduces a source of random error to the method which may be amplified by the computational algorithm[9]. Energy range and energy dependence can be improved by using a larger number of elements or thinner detectors at the expense of greater complexity and higher random error[7].

The two techniques discussed above use conventional heating in which a TLD chip was brought into mechanical contact with a heated metal plate or immersed in a hot gas or fluid. Heating rates were limited to about 10 $K.s^{-1}$. In recent years the use of laser beams to heat TLD chips has been studied as a direct, rapid and noncontact heating method[10,11,12], providing a high heating rate of about 10^4 $K.s^{-1}$. Laser heating has been recognized as a promising technique to increase the signal-to-noise ratio[13], because the dark current background noise reduces proportionally to the reduction in time achieved over conventional heating. This paper presents a computational study of a new method of extracting depth-dose distribution (between the surface and the depth at 1.0 $g.cm^{-2}$) from a thick TLD chip using pulsed laser heating schemes. This depth-dose distribution provides

not only the information about shallow (or skin) and deep doses, but also the dose at the depth of 300 $mg.cm^{-2}$ (the depth of the lens).

METHODS

The original hypothesis of this study was that a thick TLD (>0.1 cm) may be used to determine shallow and deep doses in mixed radiation dosimetry using the differential heating technique[14], which employs a focused laser beam to selectively heat the superficial and the deep portions of the TLD. This approach was then extended to the pulsed laser heating technique, in which a sequence of laser pulses with various powers and durations is applied to a TLD. The resulted temporal output of TL signal contains depth-dose information, which can be extracted by iterative unfolding techniques.

Figure 1 describes the conceptual thick TLD, which is a parallelepiped LiF chip measuring 0.3 cm on its sides and 0.38 cm on its height. The main feature of this dosemeter is that the shallow and deep doses correspond to the thicknesses of 0.0027 cm (7 $mg.cm^{-2}$) and 0.38 cm (1000 $mg.cm^{-2}$), respectively. The computational study includes various numerical and analytical methods used to simulate and optimize the performance of the proposed TLD system. Figure 2 provides the logistics of the computational study. The idea is based on the fact that the depth-dose distribution in a TLD may be unfolded from a collection of TL light emissions following the heating with a sequence of laser pulses. The unfolding is possible because one may select a particular heating scheme (i.e. a sequence of laser pulses, each with a specific power, duration, and cooling period) so that each pulse preferentially extracts TL light from a certain depth in a TLD. As illustrated in Figure 2, the temperature profile of a TLD was first obtained by solving the

heat conduction equation with a specific heating scheme. The TL light intensity vs. time (or the glow curve) was then calculated using a first-order kinetic model and an initially guessed depth-dose distribution. The TL light thus obtained was then used with the response function matrix of the TLD to update the depth-dose distribution. This iterative procedure continues until the depth-dose distributions between two consecutive iterations converges to a preset deviation criterion. Several computer programs were developed based on the computational methods. In order to computationally evaluate the performance of various pulsed laser heating schemes, depth-dose distributions for all the DOELAP radiation fields[15] for dosemeter calibration were calculated by the Monte Carlo electron/photon transport code EGS4[16]. These depth-dose distributions were then used to generate TL light (or the glow curve) for each heating scheme. Many pulsed laser heating schemes were studied for all the DOELAP radiation fields, and the resulting unfolding depth-dose distributions were then compared with that obtained by the EGS4. The judgment for the optimal heating scheme was based on how good the agreement is between the unfolded depth-dose distributions and the distributions obtained by EGS4. Another requirement for an optimal heating scheme is that it should be fairly simple to implement. More detailed calculational methods are described in the following subsections.

Heat Conduction Calculations

The transient temperature profiles of the thick TLD during and after an uniform surface heating by a laser pulse was calculated by numerically solving the following heat conduction equation:

$$\rho C_p \frac{\partial T}{\partial t} = k(T)\nabla^2 T + \frac{\partial k}{\partial T}[(\frac{\partial T}{\partial x})^2 + (\frac{\partial T}{\partial y})^2 + (\frac{\partial T}{\partial z})^2] + S \qquad (1)$$

where ρ is the density, C_p is the specific heat capacity, k is the thermal conductivity, and S is the heat source function, i.e. the power per unit volume present at a depth z during laser heating. Correcting for reflective loss on the front surface at z=0, the heat source function becomes

$$S(z) = \mu(1 - R_f)I_0 e^{-\mu z} \qquad (2)$$

where z is the depth in TLD, R_f is the reflectivity, μ is the absorption coefficient of laser beam, and I_0 is the beam power density. The expression of Equation (1) specifically considers the temperature dependencies of thermal conductivity, i.e. k(T), which varies considerably for temperatures between 0° and 500° C. The temperature dependence of the thermal conductivity was assumed to follow T^{-1} relationship[17]. With a uniform heating at the TLD surface (i.e. at z=0) and a zero-heat-flux condition at the side boundaries, Equation (1) can be simplified to a 1-dimensional problem. The solution of Equation (1) was obtained numerically using the explicit technique[18] in which the entire TLD was discretized into a large number of depth intervals.

Calculation of Depth-Dose Distributions by EGS4

Depth-dose distributions for all the DOELAP radiation fields (listed on Table 1) for dosemeter calibration were calculated by the Monte Carlo code EGS4. The TL material used in EGS4 is LiF, and the all incident particles were assumed to be perpendicular to the front surface of the TLD. 50,000 particles were run for every EGS4 calculation for every

DOELAP radiation field. For the mixed fields listed on Table 1, a 1:1 mixing ratio was applied. The calculated depth-dose distributions were then used with the temperature profiles (provided by heat conduction calculations) to generate glow curves.

Glow Curve Calculation

Glow curves of a TLD following pulsed laser beam heating were calculated numerically by integrating the TL light intensities of all the depth intervals. For a depth-dose distribution, D(z), the resulting TL light intensity corresponding to the i^{th} pulse of a heating scheme can be expressed as

$$I_i = \int_{t_i} \int_0^L D(z) R_i(z,t) dz dt \qquad (3)$$

where t_i is the duration of the i^{th} pulse, L is the TLD thickness, and $R_i(z,t)$ is the response function converting the depth-dose distribution to TL light intensity. In this study, $R_i(z,t)$ was calculated based on the uniform depth-dose distribution. The glow curve peaks considered in this study are commonly called peaks 2,3,4, and 5 (as shown in Figure 3), corresponding to the trap depths of 1.13, 1.23, 1.54, and 2.17 eV and frequency factors of 6.1×10^{13}, 4.0×10^{13}, 7.3×10^{15}, and 4.0×10^{21} sec^{-1} via a fit of experimental curves to first-order kinetics described by MeKeever[19]. Laser heating generates a time-dependent temperature profile in the TLD. The TL light intensity is a function of temperature T, and it was calculated by the first-order kinetic expression

$$I(T) = cn_0 s_0 \exp[-\frac{E}{k_b T}] \exp\{-\frac{s_0}{b} \int_{T_0}^{T} \exp[-\frac{E}{k_b T}] dT\} \qquad (4)$$

where T is the absolute temperature, n_0 is the concentration of initially trapped charges, s_0 is the frequency factor, E is the activation energy (or trap depth), k_b is the Boltzmann's constant, and b is the heating rate (i.e. dT/dt, assuming it is linear).

Because it was speculated[20] that the frequency factors decrease in proportion to the increase of heating rate, and because the heating rate with the laser beam is approximately 100 times that used by McKeever[19], the glow curves in this study were calculated with the afforementioned frequency factors reduced by a factor of 100. Figure 4 shows the comparison between the calculated glow curve and the experimentally measured glow curve[21] for a 0.038 cm thick LiF (TLD-100) Harshaw chip with a 10 W laser of uniform beam profile. As shown, there is a general agreement between the two curves characteristically. The difference between the absolute thermoluminescent light intensities is attributed to the fact that the experimentally measured glow curve was obtained based on the TLD mounted on a glass substrate, whereas the calculated glow curve did not include this condition

Unfolding of Depth-Dose Distribution

Since in practice both I_i and $R_i(z,t)$ are known in Equation (3), the depth-dose distribution, D(z), can be obtained by solving the inverse problem of Equation (3). The method used to solve this inverse problem is based on an iterative algorithm developed by Doroshenko[22]. In order to numerically carry out the iterative algorithm, Equation (3) was first converted to the matrix form:

$$I_i = \sum_{j}^{M} D_j R_{ij} \qquad (5)$$

where D_j is the absorbed dose at j^{th} depth interval, M is the total number of discretized depth intervals in the TLD, and R_{ij} is the response function matrix which converts dose at j^{th} depth interval to TL light intensity following the heating by the i^{th} pulse. The iterative procedure follows the steps below:

(1) give an initial guess of D_j (e.g., an uniform depth-dose distribution),

(2) calculate I_i using Equation (5) for all the laser pulses in a heating scheme,

(3) update D_j with the measured I_i using:

$$D_j^{l+1} = \frac{D_j^l}{\sum_{i=1}^{N} R_{ij}} \sum_{j=1}^{M} R_{ij} \frac{I_{i,measured}}{I_{i,calculated}} \tag{6}$$

where D_j^l is the depth-dose distribution for the l^{th} iteration, and N is the total number of laser pulses, and

(4) iterate steps (2)-(4) until either a specified number of iterations is exceeded or a specified convergence criterion is met. The convergence criterion is based on the deviation of the calculated TL light intensities and the measured TL light intensities for all the laser pulses in a heating scheme. The deviation is defined by the following equation:

$$\varepsilon^l = \frac{1}{N} \sum_{k=1}^{N} [(\frac{I_{k,calculated}^l - I_{k,measured}}{I_{k,measured}})^2]^{1/2} \tag{7}$$

Due to the nature of this iterative algorithm, the final solution does vary slightly with the initial guesses of D_j. The initial guesses of D_j used for all cases in the study were an

uniform depth-dose distribution (i.e. $D_j = 1.0$), because it is most reasonable to assume such a distribution when a radiation field is practically unknown.

RESULTS AND DISCUSSION

To obtain the optimum pulsed heating schemes, a large number of heating schemes were investigated in this study[14]. These heating schemes mainly consist of combinations of various laser powers, pulse durations, and cooling periods between two consecutive pulses. Because the results for all the heating schemes are too voluminous to be presented, this section only presents the results for the optimum heating scheme. The optimum heating scheme consists of a total of 6 laser pulses. The pulse sequence started with a set of 3 pulses heating the front surface of the TLD, and then followed by another set of 3 pulses heating the back surface of the TLD. The laser powers and durations associated with each pulse, and cooling periods between two consecutive pulses are shown in Figure 5. As shown, the first pulse of a three-pulse set is always high-power and short-duration so that it preferentially heats the superficial layer of the TLD. The second and the third pulses of the three-pulse set are less-power and longer-duration so that the temperature at inner portion of the TLD can be elevated without overheating the surface. Figure 6 and Figure 7 show the calculated temperature profiles and glow curves produced by each set of three pulses, respectively, and the calculations were based on a depth-dose distribution produced by a $^{90}Sr/^{90}Y$ beta source.

Figure 8 (a)-(d) shows the unfolded depth-dose distribution and the distributions calculated by EGS4 for the TLD irradiated with various DOELAP radiation fields. All four figures show good agreements between the unfolded depth-dose distributions and the

distributions calculated by EGS4. Shallow doses, doses at 300 mg.cm^{-2}, and deep doses obtained from the unfolded depth-dose distributions were all quantitatively examined, and compared with those obtained from EGS4 calculations. The unfolded results and the EGS4-calculated results for doses at the depth of 300 mg.cm^{-2} were found to agree within 10% for all the DOELAP radiation fields. The comparison for shallow doses and deep doses are summarized in Table 2 and Table 3, respectively. Table 2 indicates that except for the fields containing ^{137}Cs, the unfolded depth-dose distribution based on the optimum pulsed laser heating scheme predicts well the shallow doses (i.e. <20% of error) for the DOELAP radiation fields. Table 3 indicates that the unfolded depth-dose distribution based on the optimum pulsed laser heating scheme predicts well the deep doses (i.e. <10% of error) for all the DOELAP radiation fields. The fields which contain ^{204}Tl shown in Table 2 are not included in Table 3 because ^{204}Tl has no contribution to deep doses. The lack of agreement of shallow doses for the fields containing ^{137}Cs is due to the sharp gradient of dose distribution on the superficial layer. The sharp gradient cannot be accurately resolved by the few more-or-less smoothly distributed response functions. The lack of agreement of shallow doses, however, should not be thought as a drawback for the proposed technique, because deep dose (which is accurately predicted) is usually the limiting factor for the fields containing ^{137}Cs.

Due to the uncertainties associated with the response functions and the experimental data, the unfolded results are subjected to variations. The variations of unfolded depth-dose distributions due to the uncertainties associated with TLD thermal parameters (i.e., absorption coefficient, thermal conductivity, and specific heat) were systematically

studied[14]. As examples, Figure 9 (a) and (b) show the variations of unfolded depth-dose distribution in the TLD due to 5% variations of thermal conductivity and specific heat, repectively. The TLD was exposed to a 20 keV x-rays. Table 4 shows the relative errors (%) of shallow and deep doses unfolded from the thick TLD with respect to ±2% and ±5% variations of the three thermal parameters. The corresponding errors of unfolded doses are between 4.3% and 50.9%. In addition, shallow doses are significantly more sensitive to the variations of thermal parameters than are the deep doses. Among the three thermal parameters, the unfolded doses are most sensitive to the specific heat.

The low dose threshold for the thick TLD were not included in this computational study. Due to the larger quantity of TL material, one may expect the thick TLD to have lower dose threshold than that of thin TLDs. The thermal quenching effect caused by the high laser heating rate, however, may diminish this claim. To thoroughly address this issue, an experimental study must be conducted.

ACKNOWLEDGMENT

This work was supported by the U.S. Department of Energy contract No. DE-FG02-92ER75703.

REFERENCES

1. *International Commission on Radiological Protection Publication No. 26 Recommendations of the International Commission on Radiological Protection.* (Oxford:Pergamon Press) (1977).

2. *International Commission on Radiation Units and Measurements Publication No. 39 Determination of Dose Equivalents Resulting from External Radiation Sources.* (Bethesda: ICRU) (1985).

3. Wu, F. Zha, Z. Li, J. and Zhu, Z. *LiF(Mg,Cu,P) Thin Dosemeter for Skin Dose Measurement.* Radia. Prot. Dosim. **33**, 331-334 (1990).

4. Hoffman, J. Tetzlaff, W. Hegland, J. Bloomsburg, C. and Braunlich, P. *Development of Thin Layer Ceramic TLD Chips.* Radia. Prot. Dosim. 47, 489-491 (1993).

5. Sherbini, S. Sykes, J. Lodd, G. and Porter, S. W. *The Use of Multi-Element TL Dosimeters for Beta and Mixed Beta/Gamma Personnel Monitoring.* Proc. Int. Beta Dosimetry Symp. Washington, D.C.: NUREG/CP-0050, 569-575 (1983).

6. Gesell, T.F. Jones, D.E. Gupta, V.P. Kalbeizer, F.L. and Cusomano, J.P. *Personnel Beta-Dosimetry Method for Reducing Energy Dependence.* IDO-12090. (Dosimetry Branch, Radiological and Environmental Sciences, U.S. Department of Energy, Idaho Falls, Idaho 83401) (1979).

7. Christensen, P. *Review of Personal Monitoring Techniques for the Measurement of Absorbed Dose from External Beta and Low Energy Photon Radiation.* Radia. Prot. Dosim. **14**, 127-135 (1986).

8. Stanford, N. and McCurdy, D.E. *A Single TLD Dose Algorithm to Satisfy Federal Standards and Typical Field Conditions.* Health Phys. **58**, 691-704 (1990).

9. Kearfott, K.J. Han, S. McMahan, K.L. Samei, E. *Sensitivity of a Mixed Field Dosimetry Algorithm to Uncertainties in Thermoluminescent Element Readings.* Health Phys. **68**, 340-349 (1995).

10. Braunlich, P.F. Jones, S.C. Abtahi, A. and DeMurcia, M. *Heating of Continuous Thermoluminescent Layers with Localised Laser Beams*. Radia. Prot. Dosim. **6**, 83-86 (1984).

11. Moreau, Y. Gasiot, J. Marah, M. and Zangaro, R. *Laser Thermoluminescence: Thermal and Optical Aspects*. Radia. Prot. Dosim. **17**, 317-320 (1986).

12. Kearfott, K.J. Grupen-Shemansky, M.E. *Design of a Positionally Sensitive Laser-Heated Thermoluminescent Detector System*. Health Phys. **59**, 421-431 (1990).

13. Braunlich, P. *Laser-Heated Thermoluminescence Neutron Dosimetry*. Eleventh US DOE Workshop on Personnel Neutron Dosimetry, 90-106 (1991).

14. Han, S. *Mixed Field Dosimetry Using Focused and Unfocused Laser Heating of Thermoluminescent Materials*. Ph.D. Dissertation, Georgia Institute of Technology (1994).

15. DOELAP. *Handbook for the Department of Energy Laboratory Accreditation Program for Personnel Dosimetry Systems*. U.S. Department of Energy, Washington, DC, DOE/EH-0026 (1986).

16. Nelson, W.R. Hirayama, H. and Rogers, D.W.O. *The EGS4 Code System*. Standard Linear Accelerator Report. SLAC-265 (1985).

17. Petrov, B.R. Tsypkina, N.S. and Seleznev, V.E. *High Temperatures-High Pressures*. **8**, 537- 543 (1976).

18. Ozisik, M.N. Heat Conduction. John Wiley and Sons, Inc. (1980).

19. McKeever, S.W.S. *Thermoluminescence in LiF: Analysis of the Glow Curves*. Nuc. Inst. Meth. **175**, 19-20 (1980).

20. Kelly, P. Abtahi, A. Braunlich, P.F. *Laser-Stimulated Thermoluminescence, II.* J. Appl. Phys. **61** (2), 738-747 (1987).

21. Braunlich, P. *Present State and Future of TLD Laser Heating.* Radia. Prot. Dosim. **34**, 345-351 (1990).

22. Doroshenko, J.J. Kraitor, S.N. Kuzuetsova, T.V. Kushnereva, K.K. Leonov, E.S. *New Methods for Measuring Neutron Spectra with Energy from 0.4 eV to 10 MeV by Track and Activation Detectors.* Nucl. Technol. **33**, 296-304 (1977).

Table Captions

Table 1. DOELAP radiation fields for dosemeter calibration[15]. These radiation fields were used to calculate the depth-dose distributions within the thick TLD by EGS4 code.

Table 2. Comparison of the unfolded results of shallow doses based on the optimum pulsed laser heating scheme and the results calculated by EGS4[16] for various DOELAP radiation fields[15].

Table 3. Comparison of the unfolded results of deep doses based on the optimum pulsed laser heating scheme and the results calculated by EGS4[16] for various DOELAP radiation fields[15].

Table 4. The relative errors (%) of shallow and deep doses unfolded from the thick TLD with respect to ±2% and ±5% variations of the three thermal parameters.

Figure Captions

Figure 1. The configuration of the thick LiF thermoluminescent dosimeter used in the pulsed laser heating study.

Figure 2. The schematic diagram of the logistics of the computational study.

Figure 3. Thermoluminescence glow curves of LiF (TLD-100) analyzed by McKeever[19]. The curves were obtained by experimental fits of LiF glow peaks (i.e. peaks 2-5), notably the trap depths of 1.13, 1.23, 1.54, and 2.17 eV and frequency factors of 6.1×10^{13}, 4.0×10^{13}, 7.3×10^{15}, and 4.0×10^{21} sec^{-1}.

Figure 4. A comparison between the calculated glow curve (solid line) and the experimentally measured glow curve (dotted line) for a 0.038 cm thick LiF (TLD-100) Harshaw chip heated by a 10 W laser of uniform beam profile. The measured glow curve was obtained from Braunlich[21].

Figure 5. Description of the optimum pulsed laser heating scheme. It consists of two sets of sequential laser pulses. (a): the first set of three laser pulses heating the front surface of the TLD, and (b): the second set of three laser pulses heating the back surface the TLD.

Figure 6. The calculated temperature profiles of the thick TLD following the optimum pulsed laser heating. (a) corresponds to the temperature profiles immediately following each of the first three laser pulses heating the front surface of the TLD, and (b) corresponds to the temperature profiles immediately following each of the second three laser pulses heating the back surface of the TLD.

Figure 7. The calculated glow curves of the thick TLD exposed with $^{90}Sr/^{90}Y$ beta particles based on the optimum pulsed laser heating scheme. (a) corresponds to the glow curve based on the first three laser pulses heating the front surface of the TLD, and (b) corresponds to the glow curve based on the second three laser pulses heating the back surface of the TLD.

Figure 8. Comparison of the depth-dose distributions in the TLD obtained from the unfolding method and that obtained by EGS4[16] for various DOELAP radiation fields[15]: (a) $^{90}Sr/^{90}Y$ beta particles, (b) ^{137}Cs photons, (c) M150 + ^{204}Tl mixed field, and (d) M30 + ^{137}Cs mixed field. The particles were assumed to be perpendicularly incident upon the front surface of the TLD.

Figure 9. The variations of unfolded depth-dose distribution in the TLD due to 5% variations of: (a) thermal conductivity and (b) specific heat. The TLD was exposed to a 20 keV x-rays.

Radiation Field	Description
K16	16 keV monoenergetic x-rays
M30	20 keV NBS filtered x-rays
S60	36 keV NBS filtered x-rays
M150	70 keV NBS filtered x-rays
H150	120 keV NBS filtered x-rays
K59	59 keV monoenergetic x-rays
^{137}Cs	662 keV Cs-137 gammas
$^{90}Sr/^{90}Y$	2300 keV (max) Sr/Y-90 betas
^{204}Tl	760 keV (max) Tl-204 betas
M30 + ^{204}Tl	20 keV x-rays + 760 keV (max) betas
S60 + ^{204}Tl	36 keV x-rays + 760 keV (max) betas
M150 + ^{204}Tl	70 keV x-rays + 760 keV (max) betas
H150 + ^{204}Tl	120 keV x-rays + 760 keV (max) betas
^{137}Cs + ^{204}Tl	662 keV gammas + 760 keV (max) betas
M30 + ^{137}Cs	20 keV x-rays + 662 keV gammas
S60 + ^{137}Cs	36 keV x-rays + 662 keV gammas
M150 + ^{137}Cs	70 keV x-rays + 662 keV gammas
H150 + ^{137}Cs	120 keV x-rays + 662 keV gammas
M30 + $^{90}Sr/^{90}Y$	20 keV x-rays + 2300 keV (max) betas
S60 + $^{90}Sr/^{90}Y$	36 keV x-rays + 2300 keV (max) betas
M150 + $^{90}Sr/^{90}Y$	70 keV x-rays + 2300 keV (max) betas
H150 + $^{90}Sr/^{90}Y$	120 keV x-rays + 2300 keV (max) betas
^{137}Cs + $^{90}Sr/^{90}Y$	662 keV gammas + 2300 keV (max) betas

Radiation Field[†]	EGS4[‡] Results	Unfolded Results	Relative Error[*] (%)
K16	2.73[**]	2.77[**]	1.47
M30	1.86	1.84	1.08
S60	0.57	0.55	3.51
M150	0.27	0.32	18.50
H150	0.44	0.37	15.90
K59	0.27	0.29	7.41
^{137}Cs	0.38	0.67	81.50
$^{90}Sr/^{90}Y$	291.0	247.4	14.98
^{204}Tl	422.9	365.9	13.48
M30 + ^{204}Tl	424.7	364.8	14.10
S60 + ^{204}Tl	423.4	364.6	13.89
M150 keV + ^{204}Tl	423.2	364.9	13.78
H150 keV + ^{204}Tl	423.3	364.5	13.89
^{137}Cs + ^{204}Tl	423.3	364.2	13.96
M30 + ^{137}Cs	2.23	2.45	9.87
S60 + ^{137}Cs	0.87	1.20	37.93
M150 + ^{137}Cs	0.65	0.98	50.77
H150 keV + ^{137}Cs	0.78	1.02	30.77
M30 + $^{90}Sr/^{90}Y$	292.9	249.0	14.99
S60 + $^{90}Sr/^{90}Y$	291.5	247.6	15.06
M150 + $^{90}Sr/^{90}Y$	291.3	247.3	15.10
H150 + $^{90}Sr/^{90}Y$	291.4	247.3	15.13
^{137}Cs + $^{90}Sr/^{90}Y$	291.4	247.9	14.93

[†] These radiation fields are described in Table 1.

[‡] These results are based on the smoothed depth-dose distributions calculated by EGS4 and, therefore, contain no uncertainty information.

[*] (Unfolded result - EGS4 result)/EGS4 result.

[**] The results correspond to the energy deposited between the depths of 5 mg/cm^2 and 10 mg/cm^2 with the unit of MeV per 0.001 cm of LiF.

Radiation Field[†]	EGS4[‡] Results	Unfolded Results	Relative Error[*] (%)
K16	0.82[**]	0.79[**]	3.7
M30	0.80	0.82	2.5
S60	0.37	0.40	8.1
M150	0.21	0.23	9.5
H150	0.37	0.36	2.7
K90	0.45	0.46	2.2
^{137}Cs	2.01	1.99	1.0
$^{90}Sr/^{90}Y$	0.11	0.10	9.1
M30 + ^{137}Cs	1.4	1.41	0.71
S60 + ^{137}Cs	1.18	1.21	2.5
M150 + ^{137}Cs	1.1	1.12	1.8
H150 + ^{137}Cs	1.18	1.16	1.7
M30 + $^{90}Sr/^{90}Y$	0.45	0.42	6.7
S60 + $^{90}Sr/^{90}Y$	0.24	0.23	4.2
M150 + $^{90}Sr/^{90}Y$	0.16	0.15	6.3
H150 + $^{90}Sr/^{90}Y$	0.24	0.22	8.3
^{137}Cs + $^{90}Sr/^{90}Y$	1.05	1.0	4.8

[†] These radiation fields are described in Table 1.

[‡] These results are based on the smoothed depth-dose distributions calculated by EGS4 and, therefore, contain no uncertainty information.

[*] (Unfolded result - EGS4 result)/EGS4 result.

[**] The results correspond to the energy deposited at the depth of 1.0 g/cm^2 with the unit of MeV per 0.001 cm of LIF.

% Variation of Thermal Parameters		Relative errors (%) of the Unfolded Results	
		Shallow Dose	Deep Dose
Absorption Coefficient	+2	9.8	2.8
	-2	-8.2	-2.4
	+5	24.5	6.8
	-5	-20.3	-6.2
Thermal Conductivity	+2	-4.3	-0.9
	-2	5.7	1.4
	+5	-11.1	-2.7
	-5	14.1	2.9
Specific Heat	+2	-14.2	-6.3
	-2	18.1	7.1
	+5	-32.1	-15.1
	-5	50.9	19.1

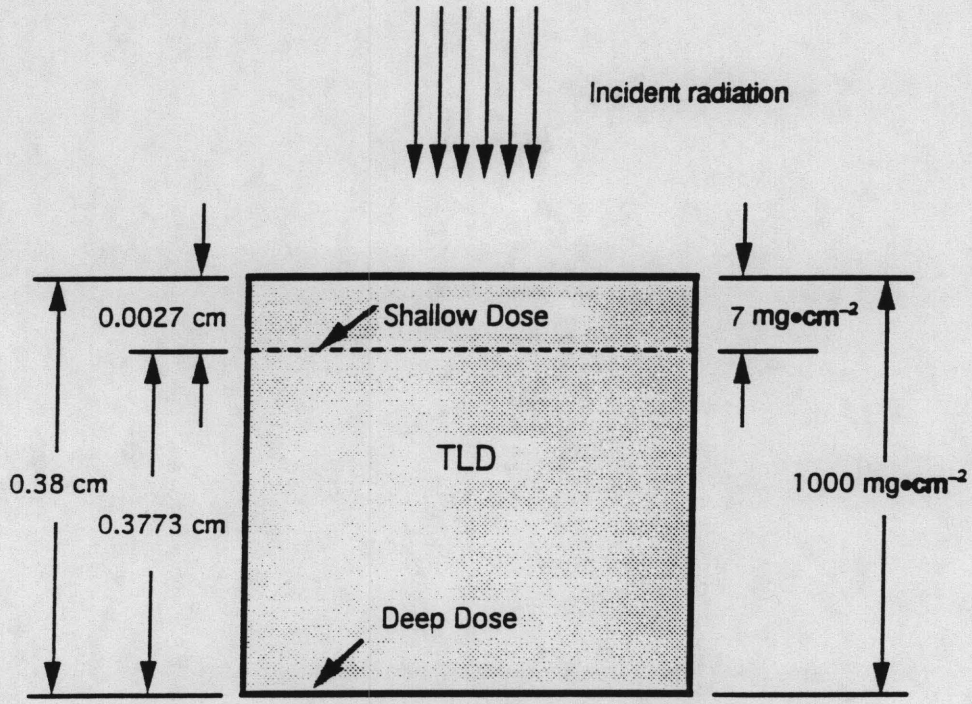
Incident radiation
0.0027 cm
Shallow Dose
7 mg•cm⁻²
TLD
0.38 cm
0.3773 cm
1000 mg•cm⁻²
Deep Dose

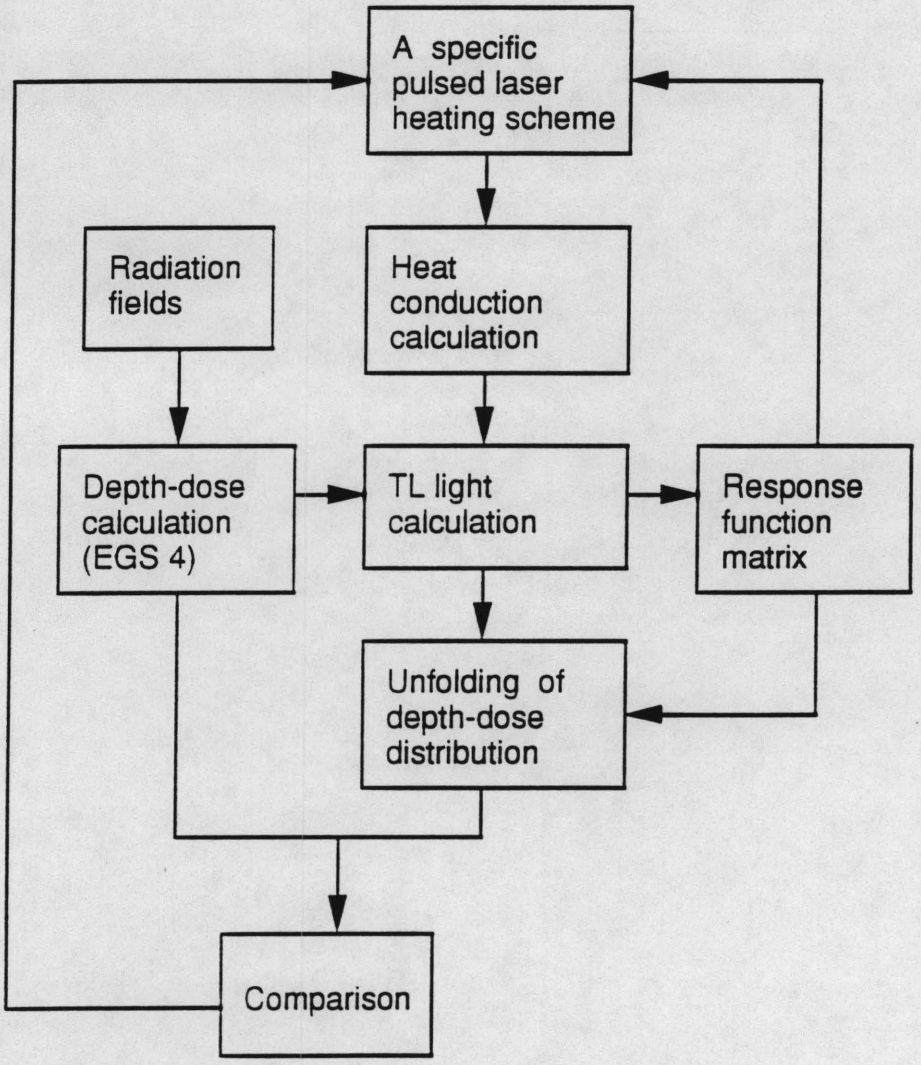
A specific pulsed laser heating scheme
Radiation fields
Heat conduction calculation
Depth-dose calculation (EGS 4)
TL light calculation
Response function matrix
Unfolding of depth-dose distribution
Comparison

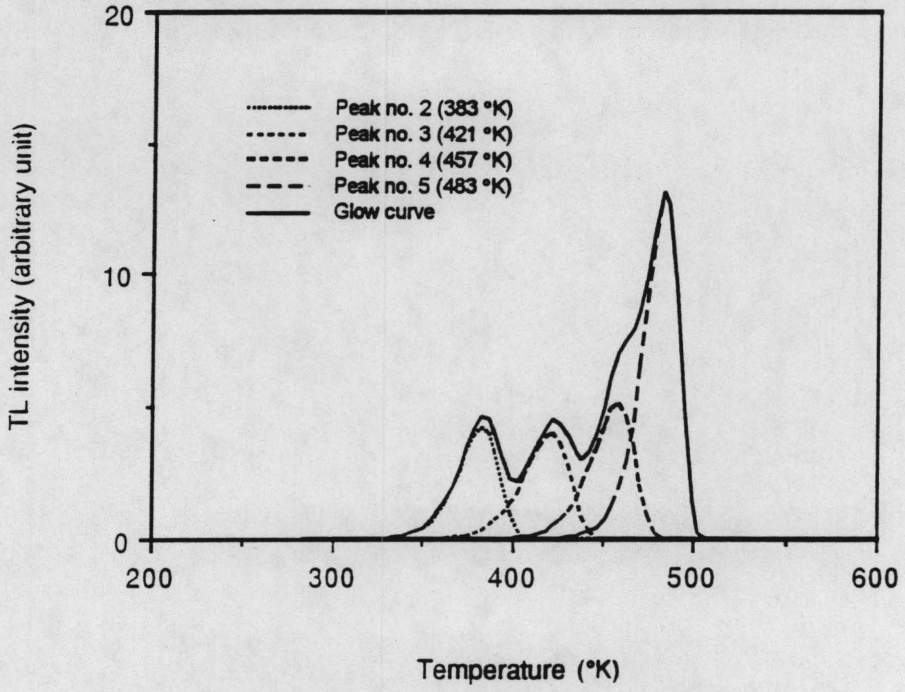
20
10
0
200
300
400
500
600
TL intensity (arbitrary unit)
Temperature (°K)
Peak no. 2 (383 °K)
Peak no. 3 (421 °K)
Peak no. 4 (457 °K)
Peak no. 5 (483 °K)
Glow curve

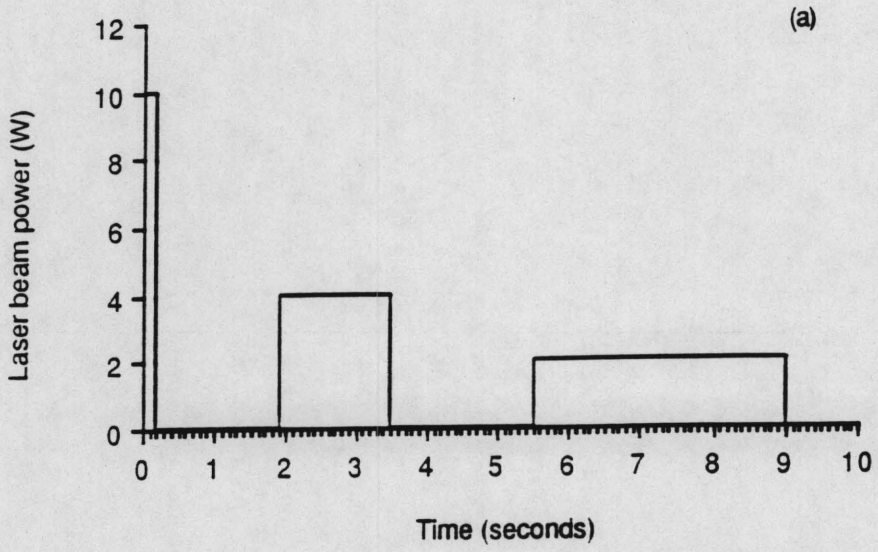
(a)
Laser beam power (W)
12
10
8
6
4
2
0
0 1 2 3 4 5 6 7 8 9 10
Time (seconds)

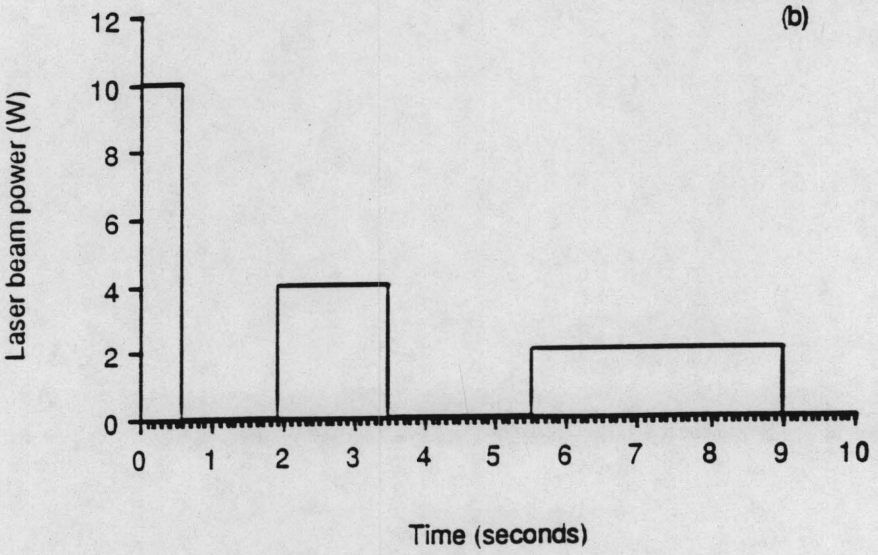
(b)
Laser beam power (W)
12
10
8
6
4
2
0
0 1 2 3 4 5 6 7 8 9 10
Time (seconds)

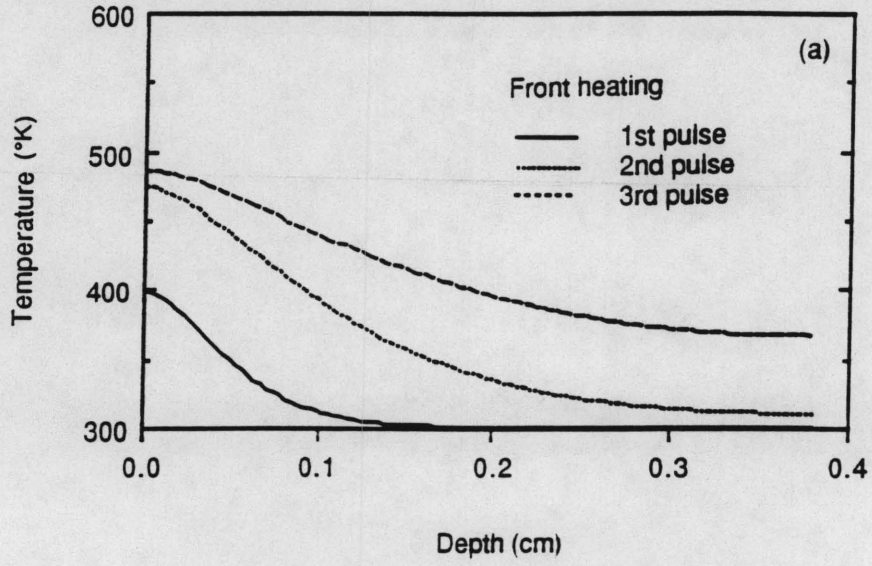
600
500
400
300
0.0
0.1
0.2
0.3
0.4
(a)
Front heating
1st pulse
2nd pulse
3rd pulse
Temperature (°K)
Depth (cm)

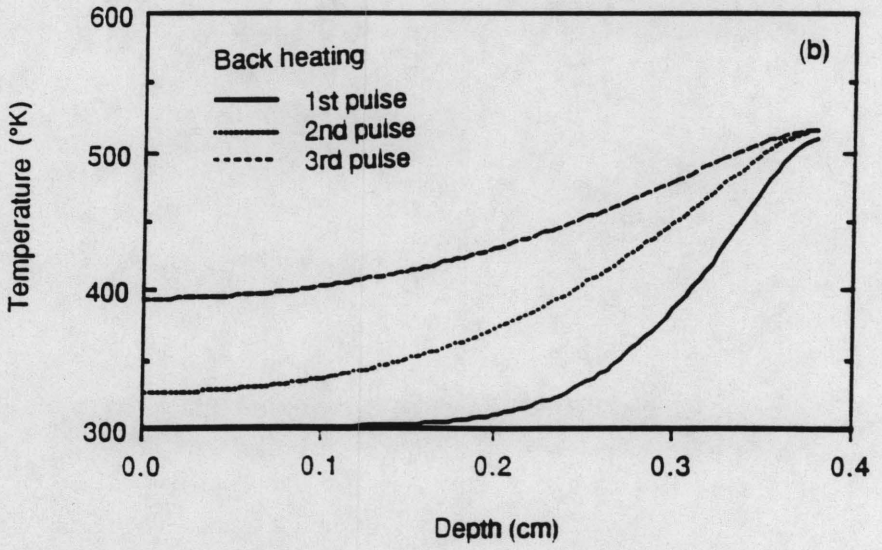
600
500
400
300
0.0
0.1
0.2
0.3
0.4
(b)
Back heating
1st pulse
2nd pulse
3rd pulse
Temperature (°K)
Depth (cm)

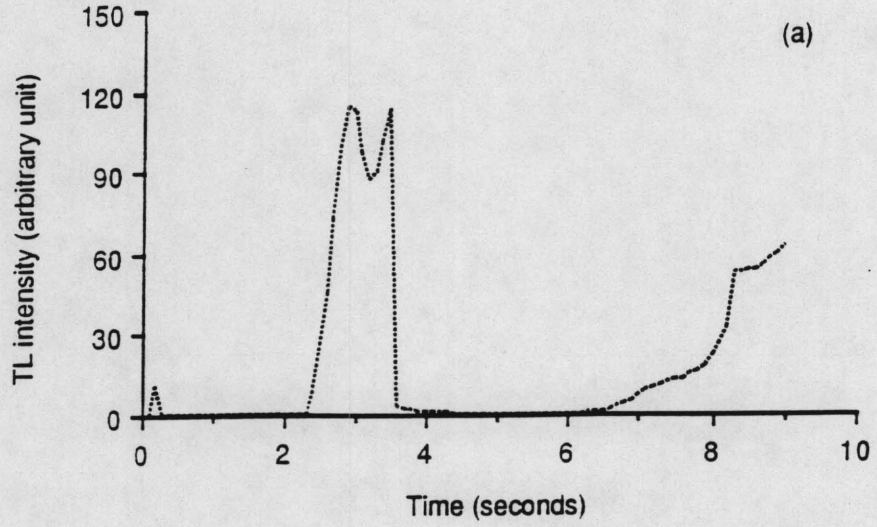
(a)
150
120
90
60
30
0
TL intensity (arbitrary unit)
0
2
4
6
8
10
Time (seconds)

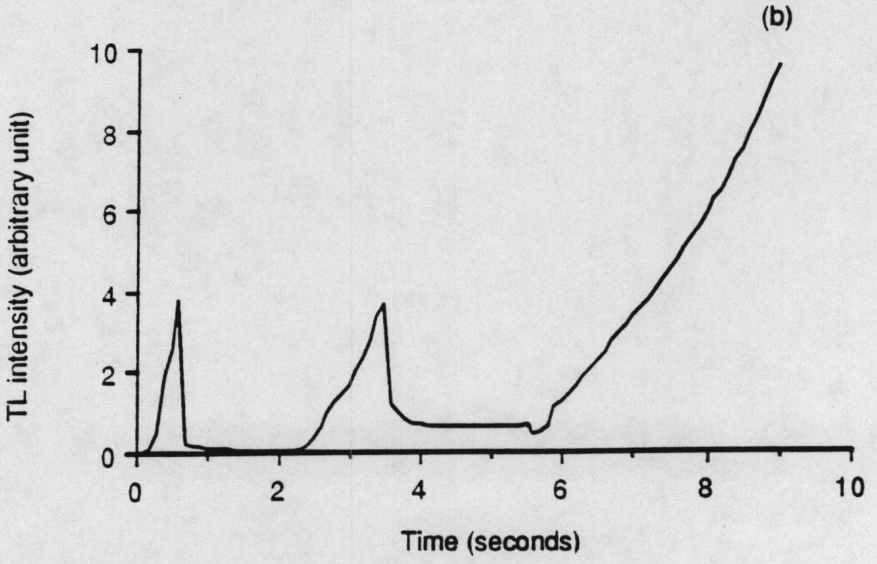
(b)
10
8
6
4
2
0
TL intensity (arbitrary unit)
0
2
4
6
8
10
Time (seconds)

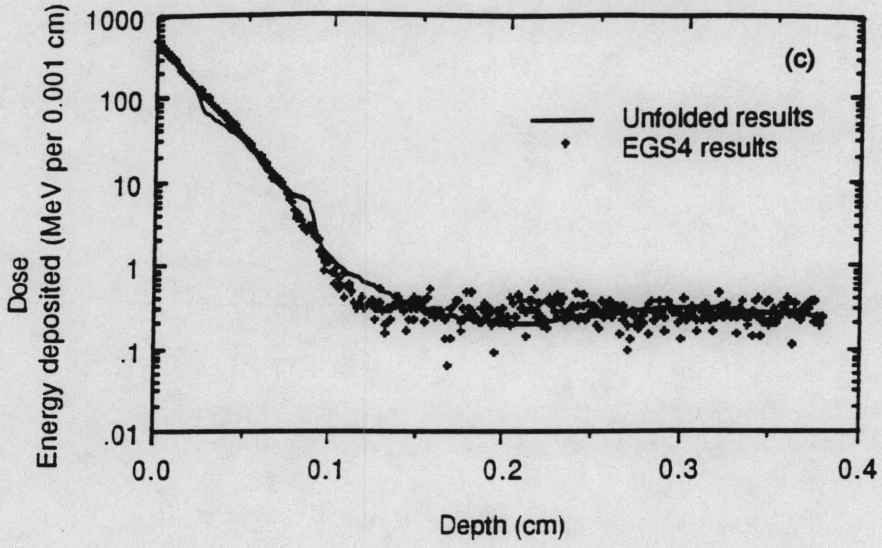
(c)
Unfolded results
EGS4 results
Dose
Energy deposited (MeV per 0.001 cm)
1000
100
10
1
.1
.01
0.0
0.1
0.2
0.3
0.4
Depth (cm)

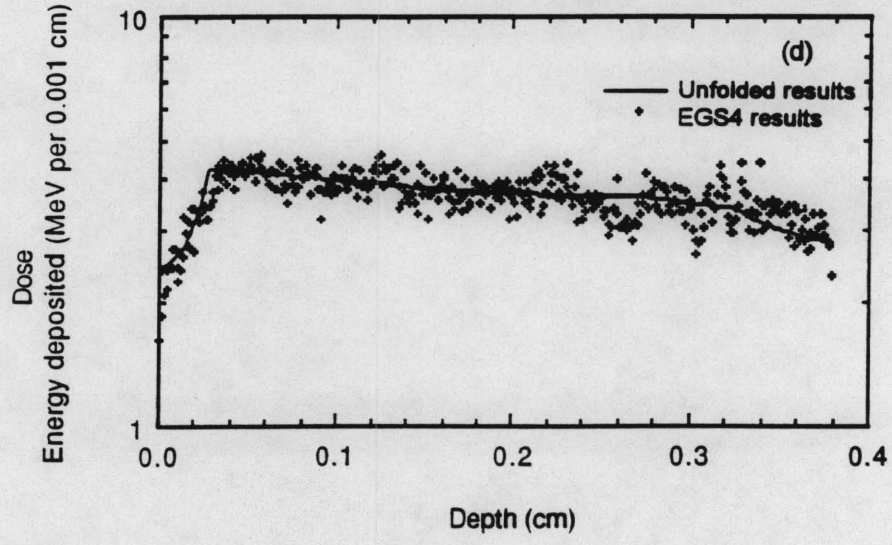
(d)
Unfolded results
EGS4 results
Dose
Energy deposited (MeV per 0.001 cm)
10
1
0.0
0.1
0.2
0.3
0.4
Depth (cm)

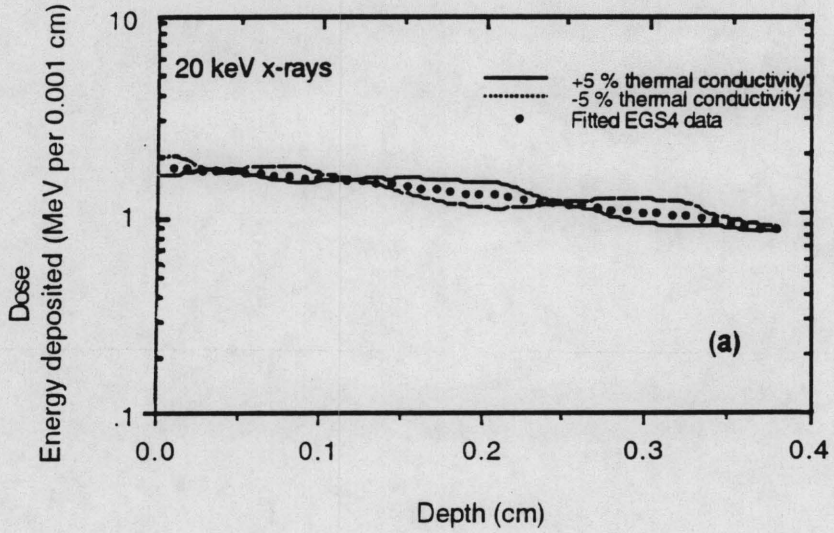
20 keV x-rays
+5 % thermal conductivity
-5 % thermal conductivity
Fitted EGS4 data
(a)
Dose
Energy deposited (MeV per 0.001 cm)
10
1
.1
0.0
0.1
0.2
0.3
0.4
Depth (cm)

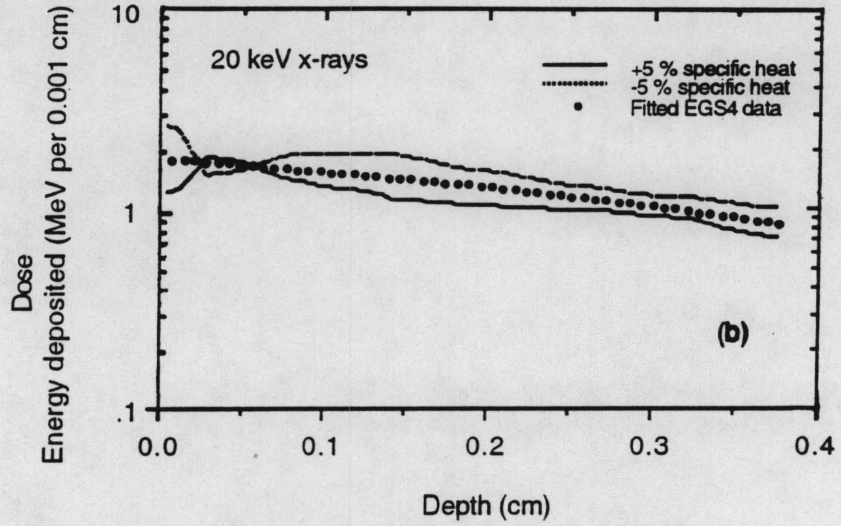
20 keV x-rays
+5 % specific heat
-5 % specific heat
Fitted EGS4 data
(b)
Dose
Energy deposited (MeV per 0.001 cm)
10
1
.1
0.0
0.1
0.2
0.3
0.4
Depth (cm)